



Endogenous Interleukin-18 Regulates Testicular Germ Cell Apoptosis during Endotoxemia

Inoue, Taketo

(Degree)

博士（保健学）

(Date of Degree)

2015-09-25

(Date of Publication)

2017-09-25

(Resource Type)

doctoral thesis

(Report Number)

甲第6486号

(URL)

<https://hdl.handle.net/20.500.14094/D1006486>

※ 当コンテンツは神戸大学の学術成果です。無断複製・不正使用等を禁じます。著作権法で認められている範囲内で、適切にご利用ください。



博士論文

Endogenous Interleukin-18 Regulates Testicular Germ Cell Apoptosis during Endotoxemia

(エンドトキシン血症時において内因性 IL-18 は
精巣生殖細胞のアポトーシスを調整する)

平成 27 年 7 月 7 日 提出

神戸大学大学院保健学研究科保健学専攻

井上 岳人

Endogenous Interleukin-18 Regulates Testicular Germ Cell Apoptosis during Endotoxemia

Abstract

Orchitis (testicular swelling) often occurs during systemic inflammatory conditions, such as sepsis. Interleukin (IL)-18 is a proinflammatory cytokine and is an apoptotic mediator during endotoxemia, but the role of IL-18 in response to inflammation in the testes was unclear. Wild type and IL-18 knockout (KO) mice were injected lipopolysaccharide (LPS) to induce endotoxemia and examined 12 and 48 hours after LPS administration to model the acute and recovery phases of endotoxemia. Caspase activation was assessed using immunohistochemistry. Protein and mRNA expression were examined by western blot and quantitative reverse-transcriptase, real-time PCR, respectively. During the acute phase of endotoxemia, apoptosis (as indicated by caspase-3 cleavage) was increased in WT mice but not in IL-18 KO mice. The death receptor-mediated and mitochondrial-mediated apoptotic pathways were both activated in the WT mice but not in the KO mice. During the recovery phase of endotoxemia, apoptosis was observed in the IL-18 KO mice but not in the WT mice. Activation of the death-receptor mediated apoptotic pathway could be seen in the IL-18 KO mice but not the WT mice. These results suggested that endogenous IL-18 induces germ cell apoptosis via death receptor mediated- and mitochondrial-mediated pathways during the acute phase of endotoxemia and suppresses germ cell apoptosis via death-receptor mediated pathways during recovery from endotoxemia. Taken together, IL-18 could be a new therapeutic target to prevent orchitis during endotoxemia.

Introduction

Infection and inflammation of the male reproductive system can disrupt spermatogenesis, induce apoptosis of testicular germ cells, cause sperm dysfunction, and obstruct the seminal pathway (Dohle *et al.* 2005, Schuppe *et al.* 2008, O'Bryan *et al.* 2000, Kajihara *et al.* 2006, Metukuri *et al.* 2010). Up to 15% of male infertility is caused by infection and inflammation (Weidner *et al.* 2013, Pellati *et al.* 2008). Several studies have indicated that failure of spermatogenesis during inflammation is caused mainly by induction of death receptor-mediated apoptosis, through the activation of death receptors including FAS and tumor necrosis factor receptor (TNFR) (Tourneur & Chiocchia 2010, Theas *et al.* 2008, Suescun *et al.* 2003, Kajihara *et al.* 2006, Theas *et al.* 2003). Because caspase-3-dependent apoptosis is ultimately activated in the germ cells, the mitochondrial-mediated apoptosis is also important (Tripathi *et al.* 2009, Otsuki 2004).

Orchitis (testicular swelling) often occurs during systemic inflammatory conditions, such as sepsis (O'Bryan *et al.* 2000, Kajihara *et al.* 2006, Metukuri *et al.* 2010). Lipopolysaccharide (LPS), the endotoxic component in the bacterial wall of Gram-negative bacteria, is a known inducer of orchitis (Kajihara *et al.* 2006, Metukuri *et al.* 2010). In an LPS-mediated orchitis mouse model, germ cell apoptosis was observed in the testes for up to five weeks after LPS injection (Kajihara *et al.* 2006). In an *Escherichia coli*-induced epididymo-orchitis rat model, severe testicular atrophy and impaired spermatogenesis were observed despite ongoing antimicrobial therapy (Demir *et al.* 2007). Understanding the mechanisms driving germ cell apoptosis caused by orchitis is important to improve spermatogenesis and male fertility after systemic inflammation. Every year 20 to 30 million people worldwide suffer from sepsis (Reinhart *et al.* 2013), and ~20% of the adult male patients suffering sepsis are 18 to 45 years old (peak reproductive ages) (Beale *et al.* 2009). Recently, long-term mortality and quality of life after sepsis has been studied (Winters *et al.* 2010), but few reports discuss the impact of sepsis on male fertility.

IL-18 is a pro-inflammatory cytokine induced by LPS in the mouse testes (Abu Elhija *et al.* 2008b). Under physiologic conditions, IL-18 regulates testicular function, development, and spermatogenesis (Strand *et al.* 2005, Abu Elhija *et al.* 2008a, Komsky *et al.* 2011). IL-18 is a mediator of apoptosis through both the death receptor (extrinsic) and the mitochondrial (intrinsic) pathways (Mariño & Cardier 2003, Zhang *et al.* 2011, Akhtar *et al.* 2011, Chandrasekar *et al.* 2004). In this study, we focused on the role of IL-18 in testicular germ cell apoptosis during sepsis by investigating IL-18-dependent effects in a mouse model of endotoxemia.

Materials and Methods

Antibodies

For Western blot analyses, rat monoclonal anti-Bid and anti-rat IgG antibodies were purchased from R&D systems (Minneapolis, MN, USA). For immunohistochemistry, polyclonal antibodies against cleaved caspase-3 (cleaved at Asp175) were purchased from Cell Signaling Technology (Danvers, MA, USA). Polyclonal antibodies against cleaved caspase-8 (Active caspase-8 antibody) were purchased from BioVison (Milpitas, MA, USA). Polyclonal antibodies specific for cleaved caspase-9 (cleaved at Asp 330) were provided by the Laboratory of Pathology, Division of Medical Biophysics, Kobe University Graduate School of Health Sciences (kindly provided by S. Kamoshida).

Animals

Male 9-10 week-old C57BL/6J (wild type; WT) mice (CLEA Japan, Tokyo, Japan) and B6.129P2-*Il18^{tm1Aki}*/J (IL-18 knock out; KO) mice (Jackson Laboratory, Bar Harbor, ME, USA) were injected with 20 mg/kg or 40 mg/kg LPS (*Escherichia coli*; O111: B4, Sigma-Aldrich, St. Louis, MO, USA) intraperitoneally. The vehicle group was injected with phosphate-buffered saline (PBS). The mice were then allowed access to a standard diet and water *ad libitum*. The testes were removed 12 hours after injection for examination of the acute phase and 48 hours after injection for examination of the recovery phase. Blood was collected at 0, 12, 24, and 48 hours after LPS injection for enzyme-linked immunosorbent assay (ELISA). This study was approved by the Institutional Animal Care and Use Committee and carried out according to the Kobe University Animal Experimentation Regulations.

Mouse Behavior

Mouse behavior was observed every hour for 48 hours after LPS or PBS injection. The severity of endotoxic shock was scored according to Rettew *et al.* (2009). Mice with ruffled fur but no detectable behavioral differences scored 1; mice with percolated fur and a huddle reflex that were still active scored 2; mice that were less active and relatively passive when handled scored 3; inactive mice that exhibited only a limited response when handled scored 4; moribund, unresponsive mice scored 5; dead mice scored 6.

Quantitative Real-Time RT-PCR

Total RNA was extracted from whole testes with ISOGEN (Nippon gene, Tokyo, Japan) according to the manufacturer's instructions. Reverse transcription was performed using iScript cDNA synthesis kits (Bio-Rad Laboratories) according to the manufacturer's instructions. The expression of *Tnf- α* , *Tnfr1*, *Fas*, *Fas ligand (Fasl)*, *Fadd*, and *iNos* were detected by quantitative real-time RT-PCR (MyiQTM Single-Color Real-Time PCR Detection System; Bio-Rad Laboratories) using SYBR green real-time PCR master mix (Table 1) (Toyobo, Osaka, Japan). Relative expression of the genes was calculated by the ddCt method after normalization to the glyceraldehyde-3-phosphate dehydrogenase (*Gapdh*).

Western Blotting

Protein was extracted from whole testes with ISOGEN (Nippon gene, Tokyo, Japan) according to the manufacturer's instruction. Equal concentrations of each pooled sample were subjected to SDS-polyacrylamide gel electrophoresis and transferred onto membranes (Amersham HybondTM-P; GE Healthcare, Buckinghamshire, UK). The membranes were blocked with 2% skim milk containing 5 mM Tris-HCl, 250 mM NaCl, and 0.1% Tween20 and incubated with primary antibodies overnight at 4°C and then incubated with secondary antibodies. Blots were developed using the ECL-plus Western Blotting Detection System (GE Healthcare) and exposed on Hyperfilm (GE Healthcare). GAPDH was used as the internal control.

Immunohistochemical Staining

Immunohistochemical staining was performed according to the method reported by Shintani *et al.* (2011). After deparaffinization, rehydration, and blocking of endogenous peroxidase, heat-induced epitope retrieval was performed in 1 mM ethylenediaminetetraacetic acid solution (EDTA, pH 8.0) when staining for cleaved caspase-3 or cleaved caspase-9 or in 10 mM citrate buffer (pH 7.0) when staining for cleaved caspase-8 for 10 min using a pressure cooker (T-FAL, Rumily, France). Nonspecific binding was blocked using Protein Block Serum Free (Dako Japan, Tokyo, Japan). The sections were incubated overnight at room temperature with the primary antibodies. To detect cleaved caspase-8 and cleaved caspase-3, the sections were incubated with the Histofine Simple Stain MAX-PO (Nichirei, Tokyo, Japan) for 1 hour at room temperature. To detect cleaved caspase-9, the sections were immunostained by Mach 3 Rabbit HRP Polymer Detection (Biocare Medical LLC, Concord, CA, US) according to the manufacturer's instructions. The reaction products were visualized with diaminobenzidine (Liquid DAB+ substrate chromogen system; Dako Japan), and counterstained with Mayer's hematoxylin.

The percent of cleaved caspase-3-positive germ cells was calculated in each tissue section by counting the number of cleaved caspase-3-positive cells and total number of cells in selected seminiferous tubules under a light microscope (x400). In each tissue section, approximately 1,000 germ cells were counted. To avoid selection bias, five fields that included the most remarkable number of cleaved caspase 3-positive germ cells were selected in each sample. Cleaved caspase-8-positive cells and cleaved caspase-9-positive cells were counted in the same area where cleaved caspase-3-positive germ cells were observed in the serial sections. In regarding to distinction between germ cell and Sertoli cell within seminiferous tubule, Sertoli cells were identified by the morphological characteristic; non-spherical-shaped cell, irregular nucleus, and one or two clear nucleoli (Russell LD *et al.* 1990).

The double immunostaining was performed to confirm co-expression of cleaved

caspase-8 and cleaved caspase-3, or cleaved caspase-9 and cleaved caspase-3. Heat-induced epitope retrieval was performed in 10 mM Tris base containing 1 mM EDTA (pH 9.0) solution for cleaved caspase-8 and in 10 mM citrate buffer (pH 7.0) for cleaved caspase-9. After blocking nonspecific binding (Super Block; ScyTek Laboratories, West Logan, UT, US), the sections were incubated overnight with the anti-cleaved caspase-8 antibody or anti-cleaved caspase-9 antibody. Bound primary antibodies were detected with Histofine Simple Stain AP (Nichirei Bioscience, Tokyo, Japan) for cleaved caspase-8 or Mach 3 Rabbit AP Polymer Detection (Biocare Medical LLC, Concord, CA, US) for cleaved caspase-9 according to the manufacturer's instructions. The reaction products were visualized with Fuchsin+ Substrate-Chromogen System (Dako, Glostrup, Denmark). And then, to recover antigenicity of cleaved caspase-3 and to block antibody cross reactivity, heat treatment was performed in 1 mM EDTA (pH 9.0) solution for 3 min. After blocking nonspecific binding, the sections were incubated overnight with anti-cleaved caspase-3 antibody followed by incubation with Histofine Simple Stain AP. The reaction products were visualized with PermaBlue Plus/AP (Diagnostic BioSystems, Pleasanton, CA, USA). The double-immunostained sections failed to discriminate between germ and Sertoli cells due to a lack of nuclear staining, and thus were not used for counting the positive cells.

ELISA and FACSArray

Plasma IL-18 levels were assessed with an enzyme-linked immunosorbent assay (ELISA) kit specific for the 18 kDa bioactive form of IL-18 (MBL, Nagoya, Japan), according to the manufacturer's instructions. IL-6 and TNF- α were assayed using Cytometric Bead Array (CBA) Flex Sets (BD Pharmingen, Franklin Lakes, NJ, USA). Flow cytometric analysis was performed using BD FACSArray flow cytometer (BD Immunocytometry Systems, Franklin Lakes, NJ, USA) according to the method reported by Aoyama *et al.* (2009).

Statistical Analysis

All data are presented as the mean \pm standard deviation (SD). The survival rate was evaluated using the Kaplan-Meier method and a log-rank test. Mouse behavior score was evaluated by 2- factor ANOVA. Other comparisons were evaluated by ANOVA followed by a Tukey-Kramer post hoc test. A probability level of $p < 0.05$ was considered statistically significant.

Results

LPS administration to model the acute and recovery phases of endotoxemia

To investigate the acute phase and the recovery phase of systemic inflammation, we examined survival and behavior in WT mice after administration of either 20 mg LPS/kg (LPS-20) or 40

mg LPS/kg (LPS-40). WT mice injected with 40 mg LPS/kg showed higher mortality than mice injected with 20 mg LPS/kg, beginning ~18 hours after LPS injection (Fig. 1A). In the LPS-20 group, 50% survived 48 hours after LPS injection, while only 33% survived in the LPS-40 group. All of the mice given PBS instead of LPS survived.

There was increased morbidity, as indicated by the behavior score, in the LPS-40 group 18 hours after injection, which remained high throughout the remainder of the 48-hour observation period (Fig. 1B). The mice given the lower dose of LPS (LPS-20) experienced similar morbidity early after LPS injection, as indicated by the behavior score 12 hours after LPS injection, but were behaving normally with no signs of morbidity during the later portion of the 48-hour observation period (Fig. 1B). All of the mice given PBS instead of LPS exhibited normal behavior (score of 0) during the observation period (data not shown). These results indicate that the LPS-40 group did not recover from systemic inflammation induced by LPS injection, whereas the LPS-20 group recovered within 2 days.

To assess activation of inflammatory cascades typical of endotoxemia, we measured plasma IL-18, IL-6, and TNF- α levels in the LPS-40 and LPS-20 mice. Plasma IL-6 and TNF- α levels were significantly increased 12 hours after administration of either dose of LPS ($p < 0.01$). In the LPS-40 group, expression decreased to baseline within 24 hours (Fig. 1C). In the LPS-20 group expression decreased to baseline within 48 hours. In the LPS-40 group, plasma IL-18 levels increased in a time-dependent manner for 24 hours after treatment (Fig. 1C). Plasma IL-18 levels also increased significantly 12 hours after LPS administration in the LPS-20 group, albeit to a lesser degree than in the LPS-40 mice (Fig. 1C, D). Forty-eight hours after LPS administration, plasma IL-18 levels returned to baseline in the LPS-20 mice (Fig. 1D). Based on the mortality, morbidity, and plasma cytokines profiles observed, we used injection of 40 mg LPS/kg examined 12 hours after administration to model the acute phase of endotoxemia and 20 mg LPS/kg examined 48 hours after injection to model the recovery phase of endotoxemia when analyzing changes in the testes.

Testicular germ cell apoptosis during the acute phase of endotoxemia

To investigate whether endogenous IL-18 influences testicular germ cell apoptosis during the acute phase of endotomexia, we examined caspase-3 cleavage 12 hours after administration of 40 mg LPS/kg. In the WT mice, LPS administration significantly increased apoptosis in the testes from $2.8 \pm 1.0\%$ to $10.6 \pm 4.4\%$ (Fig. 2A, B, F). Cleaved caspase-3-positive germ cells were observed in spermatogonia and spermatocytes along the basal membrane of the seminiferous tubules. In IL-18 KO mice, LPS administration did not significantly increase apoptosis during acute phase of endotoxemia, and the percentage of cleaved caspase-3-positive cells was significantly lower in the KO mice than in WT mice 12 hours after LPS administration ($p < 0.01$; Fig. 2F). These results suggest that endogenous IL-18 promotes testicular germ cell apoptosis via caspase-3-dependent pathways during acute

inflammation.

Induction of apoptosis via the death receptor pathway during the acute phase of endotoxemia

Knowing that apoptosis was induced in the testes in an IL-18-dependent fashion during the acute phase of endotoxemia, we wished to examine activation of the death receptor pathway to understand the underlying mechanisms. We examined cleaved caspase-8 expression (a hallmark of death receptor-mediated apoptosis) and cleaved caspase-3 expression using serial sectioning and double immunostaining techniques to identify dual-positive cells indicative of apoptosis via activation of the death receptor pathway. In the WT mice, LPS administration increased the number of dual-positive cells ~8 fold, indicating death receptor-mediated apoptosis during LPS-induced acute phase of endotoxemia (Fig. 3A, B, G). LPS administration did not increase the number of dual-positive cells in the IL-18 KO mice suggesting an IL-18-dependent process (Fig. 3C, D, G).

Expression of mRNAs encoding important regulators of death receptor-mediated apoptosis (*Tnf- α* , *Tnfr1*, *Fas*, *FasL*, and *Fadd*), was assessed by quantitative real-time RT-PCR. The mRNAs for *Tnf- α* , *Tnfr1*, and *Fas* were significantly induced by LPS in WT mice but not in KO mice, indicating IL-18-dependent upregulation of these genes in response to LPS (Fig. 4A, B, C). The mRNAs for *FasL* (Fig. 4D) and *Fadd* (Fig. 4E) were significantly decreased following LPS exposure, and this decrease was significantly greater in the IL-18 KO mice (Fig. 4D, E).

Induction of apoptosis via the mitochondrial apoptosis pathway during the acute phase of endotoxemia

Next, we examined activation of the mitochondrial, or intrinsic, apoptotic pathway. The mitochondrial apoptotic pathway is regulated by members of the BCL-2 protein family: anti-apoptotic proteins inhibit cytochrome c release, whereas pro-apoptotic members stimulate cytochrome c release and promote caspase-9 cleavage/activation (Borner 2003, Tsujimoto 2003). In the testes, the BCL-2 family member BID is expressed (Tripathi *et al.* 2009). To investigate the impact of IL-18 on mitochondrial-mediated apoptosis, the protein levels of BID and truncated BID (tBID) proteins were examined. tBID protein was significantly higher in the WT mice group than in the KO mice after LPS administration (Fig. 5). The total level of BID protein (truncated and untruncated) did not differ between the groups (Fig. 5).

Caspase-9 cleavage and caspase-3 cleavage were examined using serial sectioning and double immunostaining techniques. Administration of 40 mg LPS/kg significantly increased the number of cleaved caspase-9/cleaved caspase-3 dual-positive cells in the testes of WT mice (Fig. 6A, B, G). IL-18 KO mice showed no increase in dual-positive cells (Fig. 6C, D,

G).

Because excessive NO activates the mitochondrial apoptotic pathway (Ranjan *et al.* 2004, Chan *et al.* 2005) and increased inducible nitric oxide synthase (iNOS) expression has been observed in autoimmune orchitis (Jarazo-Dietrich *et al.* 2012), we also measured *iNos* mRNA expression in the testes after LPS treatment. The mRNA expression of *iNos* was significantly induced by LPS injection in the WT mice but not in the IL-18 KO mice (Fig. 7). Taken together, these results indicate that IL-18 induced mitochondrial-mediated apoptosis during acute inflammation and suggest that IL-18 may enhance the expression of tBID and iNOS.

Testicular germ cell apoptosis during the recovery phase of endotoxemia

To investigate whether endogenous IL-18 affected testicular germ cell apoptosis during the recovery phase of endotoxemia, we examined caspase-3 cleavage 48 hours after injection of 20 mg LPS/kg. In the WT mice, increased apoptosis was not observed during the recovery phase (Fig. 8A, B, F). In contrast, in the IL-18 KO mice, apoptosis was detected during the recovery phase (Fig. 8C, D, F). Additionally, the absence of germ cells was observed in KO mice during recovery from LPS-induced endotoxemia (Fig. 8D). These results suggested that endogenous IL-18 suppresses testicular germ cell apoptosis via caspase-3-dependent pathways during the recovery from endotoxemia.

Induction of apoptosis via the death receptor pathway during the recovery phase of endotoxemia.

To investigate the influence of IL-18 on the death receptor-mediated apoptotic pathway during the recovery phase of endotoxemia, expression of cleaved caspase-8 and the mRNAs for *TNF- α* , *Tnfr1*, *Fas*, *FasL*, and *Fadd* were examined. More cleaved caspase-8/cleaved caspase-3 double positive cells were present in the IL-18 KO testes than in the WT testes during recovery from endotoxemia ($p < 0.01$; Fig. 9A-D, G). The expression of *TNF- α* mRNA tended to be higher in the LPS group than in the PBS group (both WT and KO mice), but the difference was not significant (Fig. 10A). Increased *Tnfr1* mRNA and *Fas* mRNA levels were seen only in the IL-18 KO mice 48 hours after LPS injection (Fig. 10B, C). There tended to be less *FasL* mRNA in the LPS group than in the PBS group (both WT and KO mice), but the difference was not significant (Fig. 10D). The level of *Fadd* mRNA (Fig. 10E) was reduced significantly by LPS in only WT mice. There were no differences in the expression of *iNos* mRNA protein among the groups during recovery from endotoxemia (data not shown). These results suggest that IL-18 suppresses caspase-8-activated apoptosis in testicular germ cells and reduces expression of *Tnfr1*, *Fas*, and *Fadd* during recovery from endotoxemia.

Discussion

This study demonstrated that IL-18 was required for testicular germ cell apoptosis via both death receptor-mediated, caspase-8-dependent pathways and mitochondrial-mediated, caspase-9-dependent pathways during the acute phase of endotoxemia. In contrast, during recovery from acute inflammation, IL-18 was required to prevent germ cell apoptosis. These results suggested that IL-18 has both pro-apoptotic and anti-apoptotic effects on testicular cells, depending on the inflammation stage.

We began our study by establishing a mouse model for endotoxemia. We used mortality, morbidity (as indicated by behavior score), and plasma cytokine levels to define acute and recovery phases of endotoxemia. In our model, mortality ranged from 50-67% depending on the dose of LPS administered. Mortality of patients with severe sepsis ranges from 30.6-80.4% (Silva *et al.* 2012); thus, we believe that the severity of sepsis in the model mimicked the severity of clinical sepsis.

Using this model, we observed cleaved caspase-3-positive apoptotic germ cells (both spermatogonia and spermatocytes) in WT mice during acute inflammation. This is in agreement with the data in several publications on germ cell apoptosis induced by LPS (O'Bryan *et al.* 2000), microcystins (Xiong *et al.* 2009), or mild heat (Sinha Hikim *et al.* 2003). In contrast, cleaved caspase-3-positive apoptotic germ cells were scarce in LPS-treated IL-18 KO mice during acute phase of endotoxemia. IL-18 is known to induce apoptosis via caspase-8-dependent pathway through up-regulation of FAS/FASL and TNF/TNFR in several mammalian cell types including renal tubular cells and cardiac microvascular/liver endothelial cells (Zhang *et al.* 2011, Chandrasekar *et al.* 2004, Mariño & Cardier 2003). Our results suggest that a similar mechanism is utilized in the testes following LPS treatment. TNF- α , which was released from testicular macrophages, causes apoptosis in germ cells (Theas *et al.* 2008). Moreover, IL-18 induces macrophage activation resulting in release of TNF- α by the macrophages (Bastos *et al.* 2007). Our study suggests that endogenous IL-18 enhances TNF- α and FASL expression in the testes, leading to TNFR1-, FAS-, and FADD-induced caspase-8 activation. As a result, IL-18 leads to germ cell apoptosis via caspase-8-dependent pathways during acute inflammation. Cleaved caspase-8 expression was also increased in spermatids after LPS stimulation. During terminal differentiation of sperm, apoptotic proteins are used for elimination of intercellular bridges between spermatid and the spermatid cytoplasm (Shaha *et al.* 2010). Thus we thought caspase-8 signal was important to hypoplasia of spermatids. However, we could not elucidate the effect of IL-18 on spermatid apoptosis in this study.

Endogenous IL-18 also enhanced expression of tBID. BID is cleaved by caspase-8, following activation of caspase-8 by FAS. tBID induces mitochondrial cytochrome c release (Clohessy *et al.* 2006). Therefore, up-regulation of FAS and FASL by IL-18 may influence BID activation. IL-18 was also required for iNOS induction, in accordance with the findings of a previous study (Ueno *et al.* 2005). The upregulation of iNOS increases cellular NO levels,

which leads to the breakdown of mitochondrial membrane potential and caspase-9 activation (Chan *et al.* 2005). Thus, IL-18 may promote germ cell apoptosis during acute phase of endotoxemia through multiple, convergent pathways that result in caspase-9 cleavage.

In contrast to the IL-18-dependent germ cell apoptosis seen in response to LPS treatment during acute phase of endotoxemia, deletion of IL-18 promoted apoptosis during recovery from endotoxemia. Our data suggest that IL-18 suppresses testicular germ cell apoptosis via caspase-8-dependent pathway during the recovery phase.

In mouse testes, endogenous IL-18 is produced in germ cells, Leydig cells, and resident macrophages and may regulate testicular function via autocrine/paracrine signaling (Abu Elhija *et al.* 2008b). IL-18 may also regulate spermatogenesis (Abu Elhija *et al.* 2008b, Strand *et al.* 2005, Komsky *et al.* 2011). Moreover, Strand *et al.* (2005) suggested that endogenous IL-18 derived from testicular cells may mitigate the harmful effects of infection/inflammation on spermatogenesis. Therefore, we speculate that testicular function during the recovery phase of endotoxemia in our mouse model was not regulated appropriately in the absence of IL-18, and as a result germ cell apoptosis increased.

Bamias *et al.* (2012) reported that the role of IL-18 depends on which cells secrete it. In the intestine, monocyte-derived IL-18 induced epithelial reconstitution during acute inflammation, but during chronic inflammation, lymphocyte-derived IL-18 induced epithelial injury. In the testes, endogenous IL-18 is continuously produced by the testicular cells (Strand *et al.* 2005, Abu Elhija *et al.* 2008a, Komsky *et al.* 2011). After infection, macrophages, dendritic cells and lymphocytes migrate to the testes (Jacobo *et al.* 2011). The IL-18 that promotes apoptosis during the acute phase of endotoxemia may be released from inflammatory cells that have migrated to the testes rather than by the testicular cells. We speculate that the role of IL-18 in testicular cell apoptosis may shift from pro-apoptotic to anti-apoptotic, depending on the inflammatory stage-dependent on which cells secrete IL-18.

The use of LPS-injected mice as a model of sepsis is one limitation of this study, as administration of LPS does not mimic all aspects of clinical sepsis. However, the model was highly reproducible. Therefore, even though our results may not completely explain testicular cell apoptosis during sepsis, they should be helpful in elucidating the underlying mechanisms. Another limitation was that we could not identify the contributions of individual cell types in our analyses of apoptotic pathways because whole testes were used for the expression assays. Future studies investigating the effects of IL-18 on distinct testicular cell types, such as germ cells, Sertoli cells, and Leydig cells, during endotoxemia are planned.

In conclusion, the role of endogenous IL-18 in testicular germ cell apoptosis may shift from pro-apoptotic to anti-apoptotic depending on the inflammatory stage by regulating expression of apoptotic mediators and controlling activation of caspase-3, caspase-8, and caspase-9. Taken together, these results suggest that IL-18 may be a new therapeutic target for acute orchitis. The risk of azospermia or oligospermia after orchitis may be mitigated by

controlling IL-18.

Declaration of interest

The authors declare that there are no conflicts of interest that could be perceived as prejudicing the impartiality of the research reported.

Funding

No external funding was obtained for this study and there are no potential competing interests.

Acknowledgements

I thank my collaborators, Michiko Aoyama-Ishikawa, Shingo Kamoshida, Satoshi Nishino, Maki Sasano, Nobuki Oka, Hayato Yamashita, Motoki Kai, Atsunori Nakao, Joji Kotani, and Makoto Usami. We thank Shannon Wyszomierki, PhD for editing the manuscript. This doctoral dissertation has been published in *Reproduction* in 2015 (Advance Publications; doi:10.1530/REP-14-0427).

References

- Abu Elhija M, Lunenfeld E, Eldar-Geva T & Huleihel M** 2008a Over-expression of IL-18, ICE and IL-18 R in testicular tissue from sexually immature as compared to mature mice. *Eur Cytokine Netw* **19** 15-24.
- Abu Elhija M, Lunenfeld E & Huleihel M** 2008b LPS increases the expression levels of IL-18, ICE and IL-18 R in mouse testes. *Am J Reprod Immunol* **60** 361-371.
- Akhtar S, Li X, Kovacs EJ, Gamelli RL & Choudhry MA** 2011 Interleukin-18 delays neutrophil apoptosis following alcohol intoxication and burn injury. *Mol Med* **17** 88-94.
- Aoyama M, Kotani J & Usami M** 2009 Gender difference in granulocyte dynamics and apoptosis and the role of IL-18 during endotoxin-induced systemic inflammation. *Shock* **32** 401-409.
- Bamias G, Corridoni D, Pizarro TT & Cominelli F** 2012 New insights into the dichotomous role of innate cytokines in gut homeostasis and inflammation. *Cytokine* **59** 451-459.
- Bastos KR, Barboza R, Sardinha L, Russo M, Alvarez JM & Lima MR** 2007 Role of endogenous IFN-gamma in macrophage programming induced by IL-12 and IL-18. *J Interferon Cytokine Res* **27** 399-410.
- Beale R, Reinhart K, Brunkhorst FM, Dobb G, Levy M, Martin G, Martin C, Ramsey G, Silva E, Vallet B, et al; PROGRESS Advisory Board.** 2009 Promoting Global Research Excellence in Severe Sepsis (PROGRESS): lessons from an international sepsis registry. *Infection* **37** 222-232.
- Borner** 2003 The Bcl-2 protein family: sensors and checkpoints for life-or-death decisions. *Mol Immunol* **39** 615-647.
- Chan SH, Wu KL, Wang LL & Chan JY** 2005 Nitric oxide- and superoxide-dependent mitochondrial signaling in endotoxin-induced apoptosis in the rostral ventrolateral medulla of rats. *Free Radic Biol Med* **39** 603-618.
- Chandrasekar B, Vemula K, Surabhi RM, Li-Weber M, Owen-Schaub LB, Jensen LE & Mummidi S** 2004 Activation of intrinsic and extrinsic proapoptotic signaling pathways in interleukin-18-mediated human cardiac endothelial cell death. *J Biol Chem* **279** 20221-20233.
- Clohessy JG, Zhuang J, de Boer J, Gil-Gómez G & Brady HJ.** 2006 Mcl-1 interacts with truncated Bid and inhibits its induction of cytochrome c release and its role in receptor-mediated apoptosis. *J Biol Chem* **281** 5750-5759.
- Demir A, Türker P, Onol FF, Sirvanci S, Findik A & Tarcan T** 2007 Effect of experimentally induced Escherichia coli epididymo-orchitis and ciprofloxacin treatment on rat spermatogenesis. *Int J Urol* **14** 268-272.
- Dohle GR, Colpi GM, Hargreave TB, Papp GK, Jungwirth A & Weidner W** 2005 EAU

- guidelines on male infertility. *Eur Urol* **48** 703-711.
- Jacobo P, Guazzone VA, Theas MS & Lustig L** 2011 Testicular autoimmunity. *Autoimmun Rev* **10** 201-204.
- Jarazo-Dietrich S, Jacobo P, Pérez CV, Guazzone VA, Lustig L & Theas MS** 2012 Up regulation of nitric oxide synthase-nitric oxide system in the testis of rats undergoing autoimmune orchitis. *Immunobiology*. **217** 778-787.
- Kajihara T, Okagaki R & Ishihara O** 2006 LPS-induced transient testicular dysfunction accompanied by apoptosis of testicular germ cells in mice. *Med Mol Morphol* **39** 203-208.
- Komsky A, Huleihel M, Ganaïem M, Kasterstein E, Komorovsky D, Bern O, Raziel A, Friedler S, Ron-El R & Strassburger D** 2011 Presence of IL-18 in testicular tissue of fertile and infertile men. *Andrologia* **44** 1-8.
- Mariño E & Cardier JE** 2003 Differential effect of IL-18 on endothelial cell apoptosis mediated by TNF-alpha and Fas (CD95). *Cytokine* **22** 142-148.
- Metukuri MR, Reddy CM, Reddy PR & Reddanna P** 2010 Bacterial LPS-mediated acute inflammation-induced spermatogenic failure in rats: role of stress response proteins and mitochondrial dysfunction. *Inflammation* **33** 235-243.
- O'Bryan MK, Schlatt S, Phillips DJ, de Kretser DM & Hedger MP** 2000 Bacterial lipopolysaccharide-induced inflammation compromises testicular function at multiple levels in vivo. *Endocrinology* **141** 238-246.
- Otsuki Y** 2004 Tissue specificity of apoptotic signal transduction. *Med Electron Microsc* **37** 163-169.
- Pellati D, Mylonakis I, Bertoloni G, Fiore C, Andrisani A, Ambrosini G & Armanini D** 2008 Genital tract infections and infertility. *Eur J Obstet Gynecol Reprod Biol* **140** 3-11.
- Ranjan P, Shrivastava P, Singh SM, Sodhi A & Heintz NH** 2004 Baculovirus P35 inhibits NO-induced apoptosis in activated macrophages by inhibiting cytochrome c release. *J Cell Sci* **117** 3031-3039.
- Reinhart K, Daniels R, & Machado FR; World Sepsis Day Steering Committee and the Global Sepsis Alliance Executive Board** 2013 The burden of sepsis: a call to action in support of World Sepsis Day 2013. *Rev Bras Ter Intensiva* **25** 3-5.
- Rettew JA, Huet YM & Marriott I** 2009 Estrogens augment cell surface TLR4 expression on murine macrophages and regulate sepsis susceptibility in vivo. *Endocrinology* **150** 3877-3884.
- Russell LD, Ettlin RA, Sinha Hikim AP & Clegg ED** 1990 Histological and histopathological evaluation of the testis. St. Louis, MO, USA: Cache River Press.
- Schuppe HC, Meinhardt A, Allam JP, Bergmann M, Weidner W & Haidl G** 2008 Chronic orchitis: a neglected cause of male infertility? *Andrologia* **40** 84-91.
- Shintani M, Sangawa A, Shintaku M, Yamao N, Miyake T & Kamoshida S** 2011

- Immunohistochemical analysis of cell death pathways in gastrointestinal adenocarcinoma. *Biomed Res* **32** 379-386.
- Shaha C, Tripathi R & Mishra DP** 2010 Male germ cell apoptosis: regulation and biology *Philos Trans R Soc Lond B Biol Sci.* **365** 1501–1515.
- Silva E, Cavalcanti AB, Bugano DD, Janes JM, Vallet B, Beale R & Vincent JL** 2012 Do established prognostic factors explain the different mortality rates in ICU septic patients around the world? *Minerva Anesthesiol* **78** 1215-1225.
- Sinha Hikim AP, Lue Y, Diaz-Romero M, Yen PH, Wang C & Swerdloff RS** 2003 Deciphering the pathways of germ cell apoptosis in the testis. *J Steroid Biochem Mol Biol* **85** 175-182.
- Strand ML, Wahlgren A, Svechnikov K, Zetterström C, Setchell BP & Söder O** 2005 Interleukin-18 is expressed in rat testis and may promote germ cell growth. *Mol Cell Endocrinol* **240** 64-73.
- Suescun MO, Rival C, Theas MS, Calandra RS & Lustig L** 2003 Involvement of tumor necrosis factor-alpha in the pathogenesis of autoimmune orchitis in rats. *Biol Reprod* **68** 2114-2121.
- Theas MS, Rival C, Jarazo-Dietrich S, Jacobo P, Guazzone VA & Lustig L** 2008 Tumour necrosis factor-alpha released by testicular macrophages induces apoptosis of germ cells in autoimmune orchitis. *Hum Reprod* **23** 1865-1872.
- Theas S, Rival C & Lustig L** 2003 Germ cell apoptosis in autoimmune orchitis: involvement of the Fas-FasL system. *Am J Reprod Immunol* **50** 166-176.
- Tourneur L & Chiocchia G** 2010 FADD: a regulator of life and death. *Trends Immunol* **31** 260-269.
- Tripathi R, Mishra DP & Shaha C** 2009 Male germ cell development: turning on the apoptotic pathways. *J Reprod Immunol* **83** 31-35.
- Tsujimoto Y** 2003 Cell death regulation by the Bcl-2 protein family in the mitochondria. *J Cell Physiol* **195** 158-167.
- Ueno N, Kashiwamura S, Ueda H, Okamura H, Tsuji NM, Hosohara K, Kotani J & Marukawa S** 2005 Role of interleukin 18 in nitric oxide production and pancreatic damage during acute pancreatitis. *Shock* **24** 564-570.
- Weidner W, Pilatz A, Diemer T, Schuppe HC, Rusz A & Wagenlehner F** 2013 Male urogenital infections: impact of infection and inflammation on ejaculate parameters. *World J Urol* **31** 717-723.
- Winters BD, Eberlein M, Leung J, Needham DM, Pronovost PJ & Sevransky JE** 2010 Long-term mortality and quality of life in sepsis: a systematic review. *Crit Care Med* **38** 1276-1283.
- Xiong Q, Xie P, Li H, Hao L, Li G, Qiu T & Liu Y** 2009 Involvement of Fas/FasL system in apoptotic signaling in testicular germ cells of male Wistar rats injected i.v. with

microcystins. *Toxicon* **54** 1-7.

Zhang H, Hile KL, Asanuma H, Vanderbrink B, Franke EI, Campbell MT & Meldrum KK 2011 IL-18 mediates proapoptotic signaling in renal tubular cells through a Fas ligand-dependent mechanism. *Am J Physiol Renal Physiol* **301** F171-F178.

Figure Legends

Figure 1. Establishing mouse models of acute-phase and recovery-phase endotoxemia. **A)** Survival. LPS-40, 40 mg LPS/kg-injected mice; LPS-20, 20 mg LPS/kg-injected mice. $n=6-10$ mice per group. **B)** Behavior scores of surviving LPS-injected WT mice. $n=6-10$ mice per group. Expression of inflammatory mediators in the LPS-40 (**C**) and LPS-20 (**D**) groups. Plasma IL-18 (open circle), IL-6 (closed circle), and TNF- α (square). $n=3-7$ mice per group. **, ##, ††: significant difference between at 0 hours and at 12 hours ($p<0.01$).

Figure 2. Testicular germ cell apoptosis during acute inflammation. **A)** WT/PBS, **B)** WT/LPS, **C)** KO/PBS, and **D)** KO/LPS. Cleaved caspase 3-positive cells are stained brown. **E)** Negative control (NC). Magnification: 400x. Scale bar: 50 μ m. **F)** Percent cleaved caspase-3-positive germ cells in seminiferous tubules. $n=6-7$ mice per group. **, $p<0.01$.

Figure 3. Cleaved caspase-8-dependent apoptosis in the testes during acute inflammation. Immunohistochemical staining for cleaved caspase-8 in **A)** WT/PBS, **B)** WT/LPS, **C)** KO/PBS, and **D)** KO/LPS. Cleaved caspase-8-positive cells are stained brown. Cleaved caspase-8-positive germ cells (arrows) are identified in the same area where cleaved caspase-3-positive germ cells are observed (see also Figure 2). **E)** Negative control (NC). **F)** The typical double immunostaining of cleaved caspase-8 (red) and cleaved caspase-3 (blue). A number of germ cells show co-expression of cleaved caspase-8 and cleaved caspase-3, visualized in purple color. A blue-colored germ cell expressing cleaved caspase-3 alone is also seen. Magnification: 400x. (inset, Magnification: 1000x) Scale bar: 50 μ m. **G)** Percent cleaved caspase-8/cleaved caspase-3 double positive germ cells in the seminiferous tubules. $n=6-7$ mice per group. **, $p<0.01$.

Figure 4. Death receptor mediated apoptosis in the testes during acute inflammation. Expression of the mRNAs for **A)** *Tnf- α* , **B)** *Tnfr1*, **C)** *Fas*, **D)** *FasL*, and **E)** *Fadd*. $n=6-7$ mice per group. **, $p<0.01$.

Figure 5. BID and tBID protein levels in the testes during acute inflammation. $n=6-7$ mice per group.

Figure 6. Cleaved caspase-9-dependent apoptosis in the testes during acute inflammation. Immunohistochemical staining for cleaved caspase-9 in **A)** WT/PBS, **B)** WT/LPS, **C)** KO/PBS, and **D)** KO/LPS. Cleaved caspase 9-positive cells are stained brown. Cleaved caspase-9-positive germ cells (arrows) are identified in the same area where cleaved caspase-3-positive germ cells are observed (see also Figure 2). **E)** Negative control (NC). **F)** The typical double immunostaining of cleaved caspase-9 (red) and cleaved caspase-3 (blue).

A number of germ cells show co-expression of cleaved caspase-9 and cleaved caspase-3, visualized in purple color. A blue-colored germ cell expressing cleaved caspase-3 alone is also seen. Magnification: 400x. (inset, Magnification: 1000x) Scale bar: 50 μ m. **G)** Percent cleaved caspase-9/cleaved caspase-3 double positive germ cells in the seminiferous tubules. $n=6-7$ mice per group. **, $p<0.01$.

Figure 7. *iNos*. mRNA levels in the testes during acute inflammation. $n=6-7$ mice per group. **, $p<0.01$.

Figure 8. Testicular germ cell apoptosis during recovery from acute inflammation. **A)** WT/PBS, **B)** WT/LPS, **C)** KO/PBS, and **D)** KO/LPS. Cleaved caspase-3-positive cells are stained brown. Areas lacking germ cells are indicated by arrowheads. **E)** Negative control (NC). Magnification: 400x. Scale bar: 50 μ m. **F)** Percent cleaved caspase 3-positive germ cells in the seminiferous tubules. $n=3$ mice in the LPS groups, $n=6$ mice in the PBS groups. **, $p<0.01$.

Figure 9. Cleaved caspase-8-dependent apoptosis in the testes during recovery from endotoxemia. Immunohistochemical staining for cleaved caspase-8 in **A)** WT/PBS, **B)** WT/LPS, **C)** KO/PBS, and **D)** KO/LPS. Cleaved caspase-8-positive cells are stained brown. Cleaved caspase-8-positive germ cells (arrows) are identified in the same area where cleaved caspase-3-positive germ cells are observed (see also Figure 8). Areas lacking germ cells are indicated by arrowheads. **E)** Negative control (NC). **F)** The typical double immunostaining of cleaved caspase-8 (red) and cleaved caspase-3 (blue). A number of germ cells show co-expression of cleaved caspase-8 and cleaved caspase-3, visualized in purple color. Magnification: 400x. (inset, Magnification: 1000x) Scale bar: 50 μ m. **G)** Percent cleaved caspase-8/cleaved caspase-3 double positive germ cells in the seminiferous tubules. $n=3$ mice in the LPS groups, $n=6$ mice in the PBS groups. **, $p<0.01$.

Figure 10. Death receptor-mediated apoptosis in the testes during recovery from endotoxemia. Expression of the mRNAs for **A)** *Tnf- α* , **B)** *Tnfr1*, **C)** *Fas*, **D)** *FasL*, and **E)** *Fadd*. $n=3$ mice in the LPS groups, $n=6$ mice in the PBS groups. **, $p<0.01$.

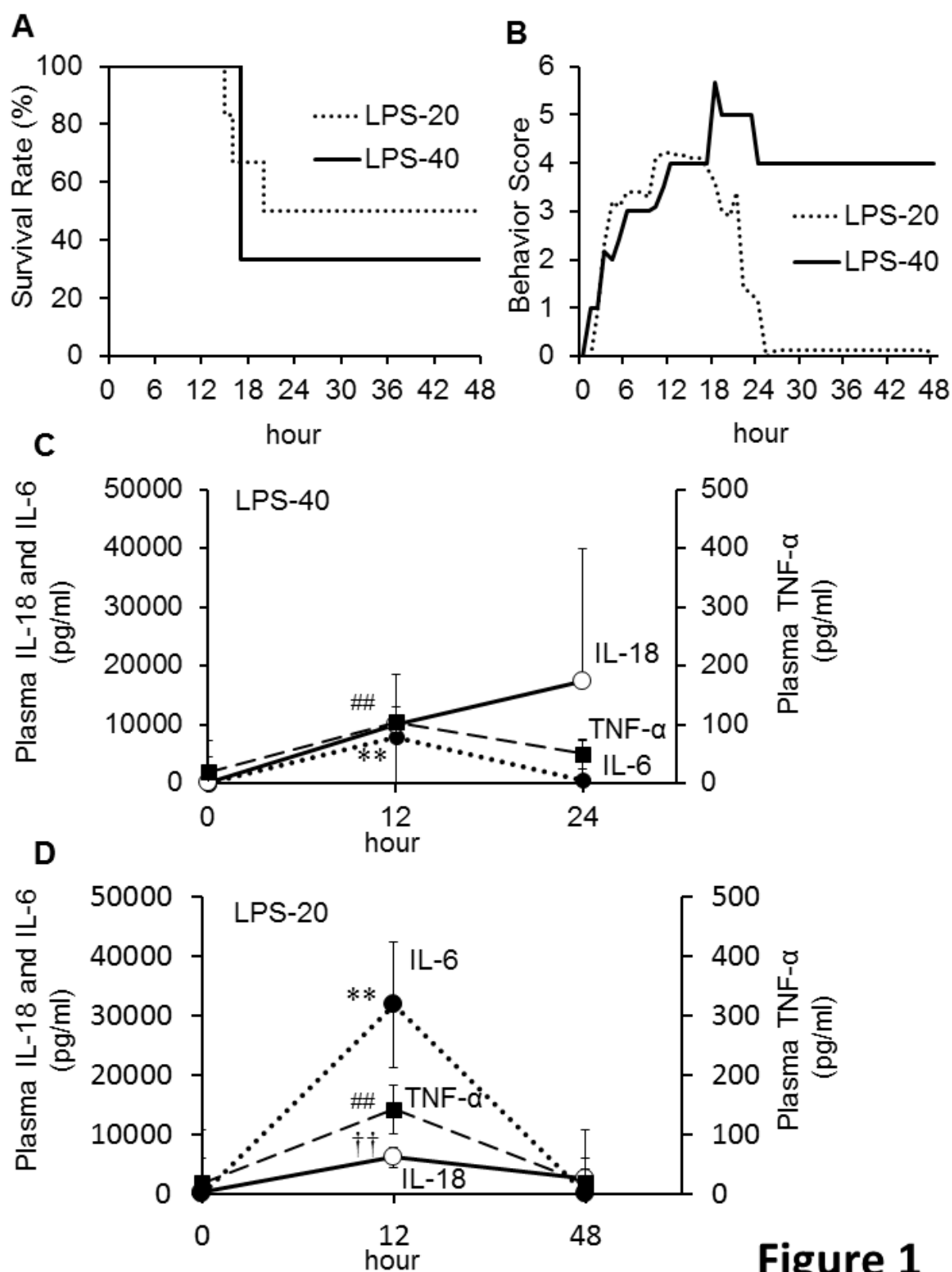


Figure 1

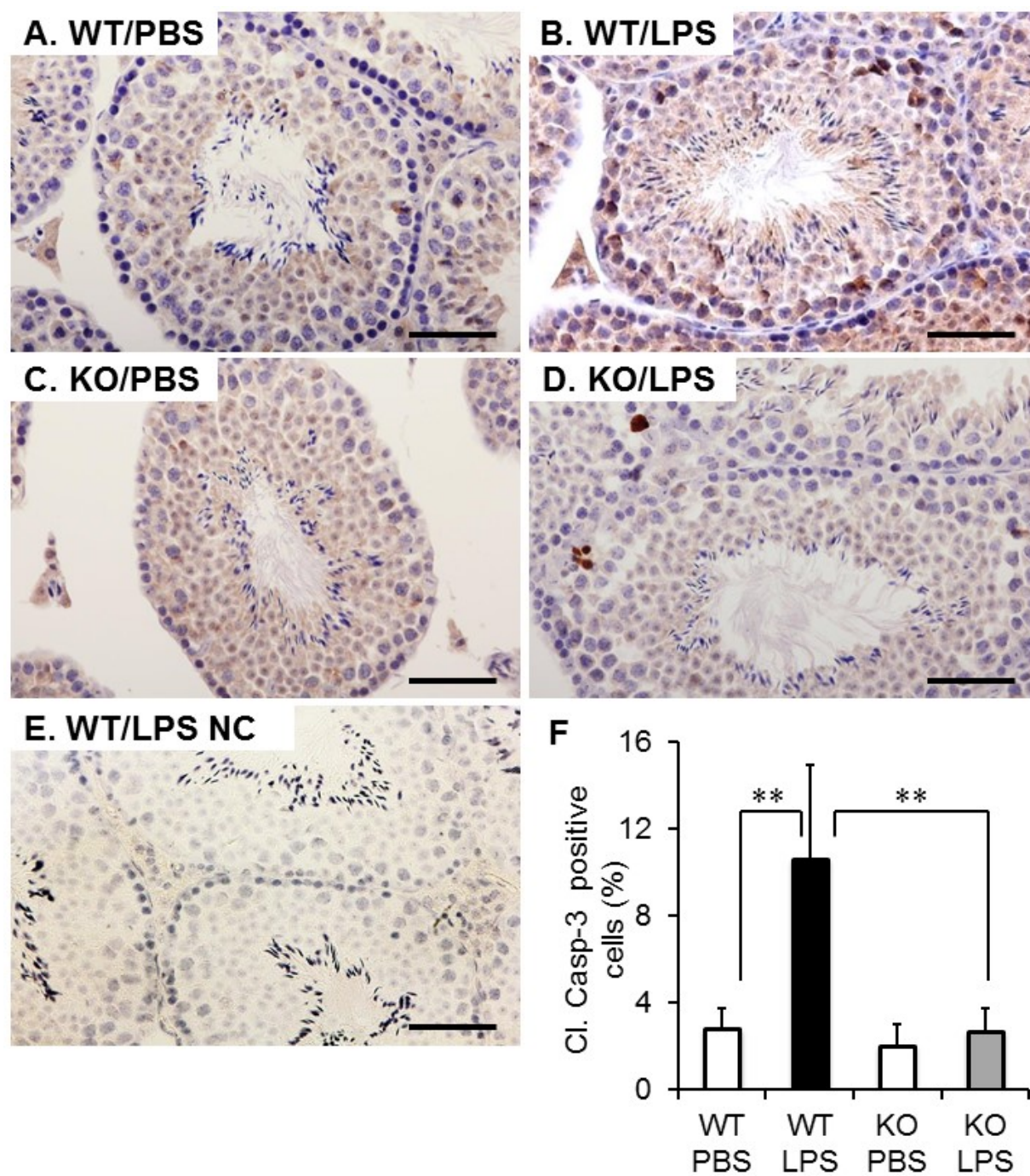


Figure 2

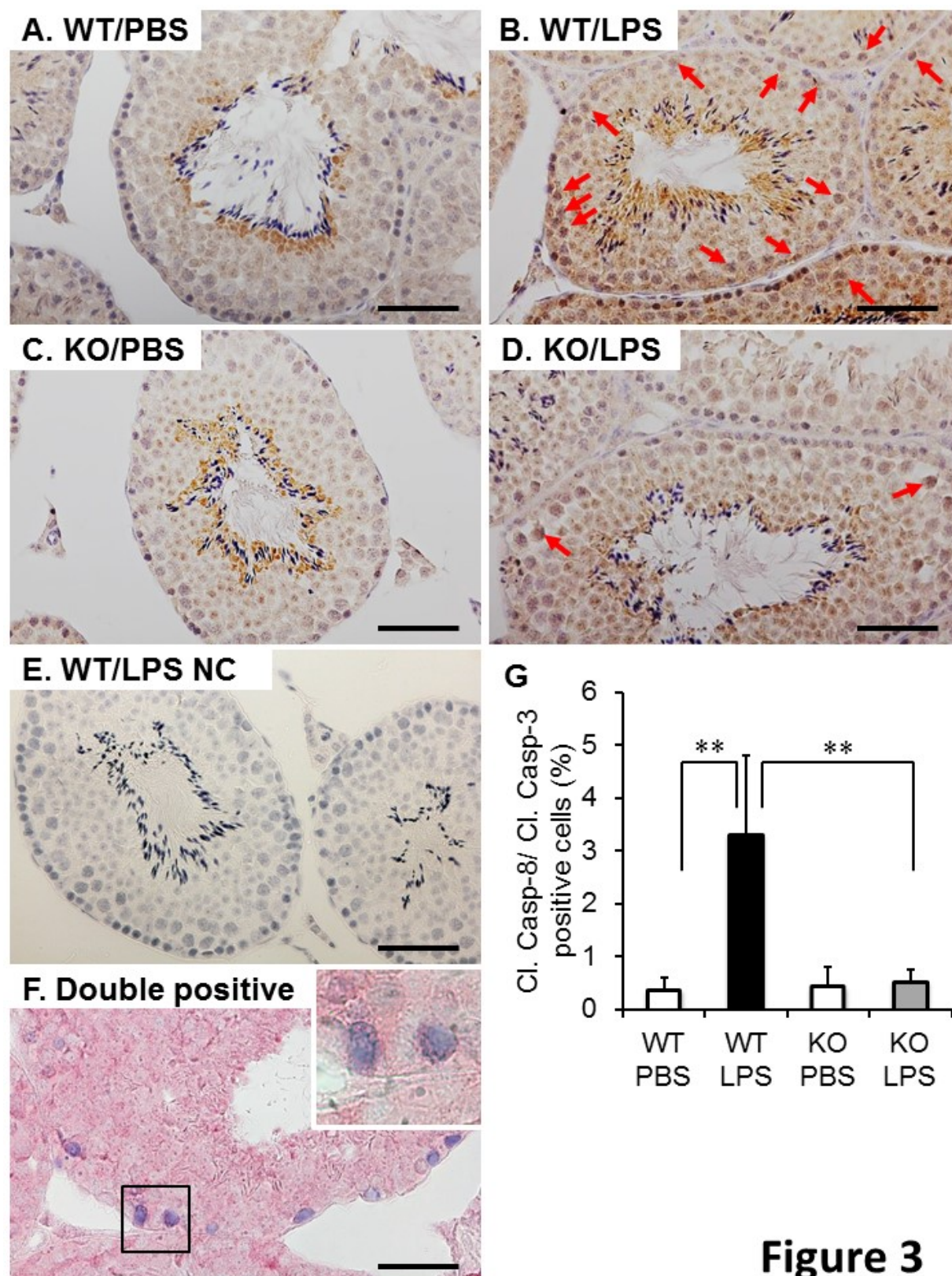
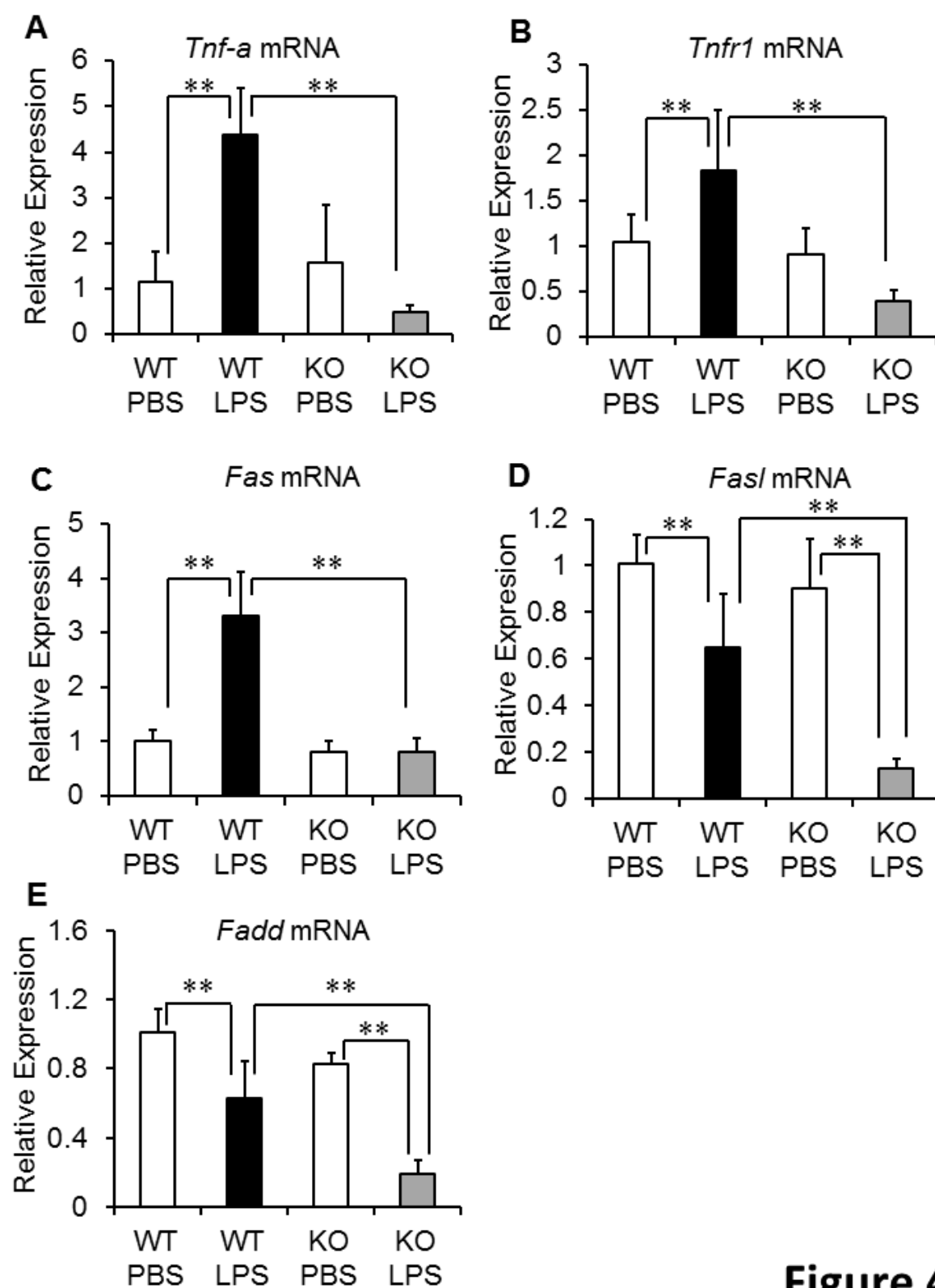
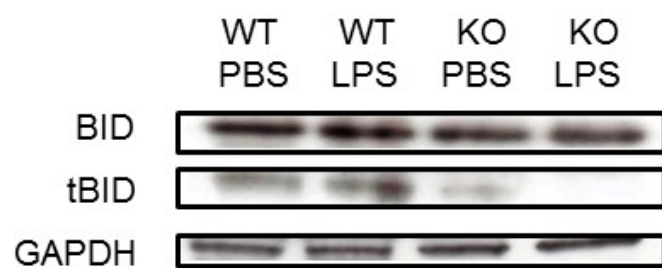
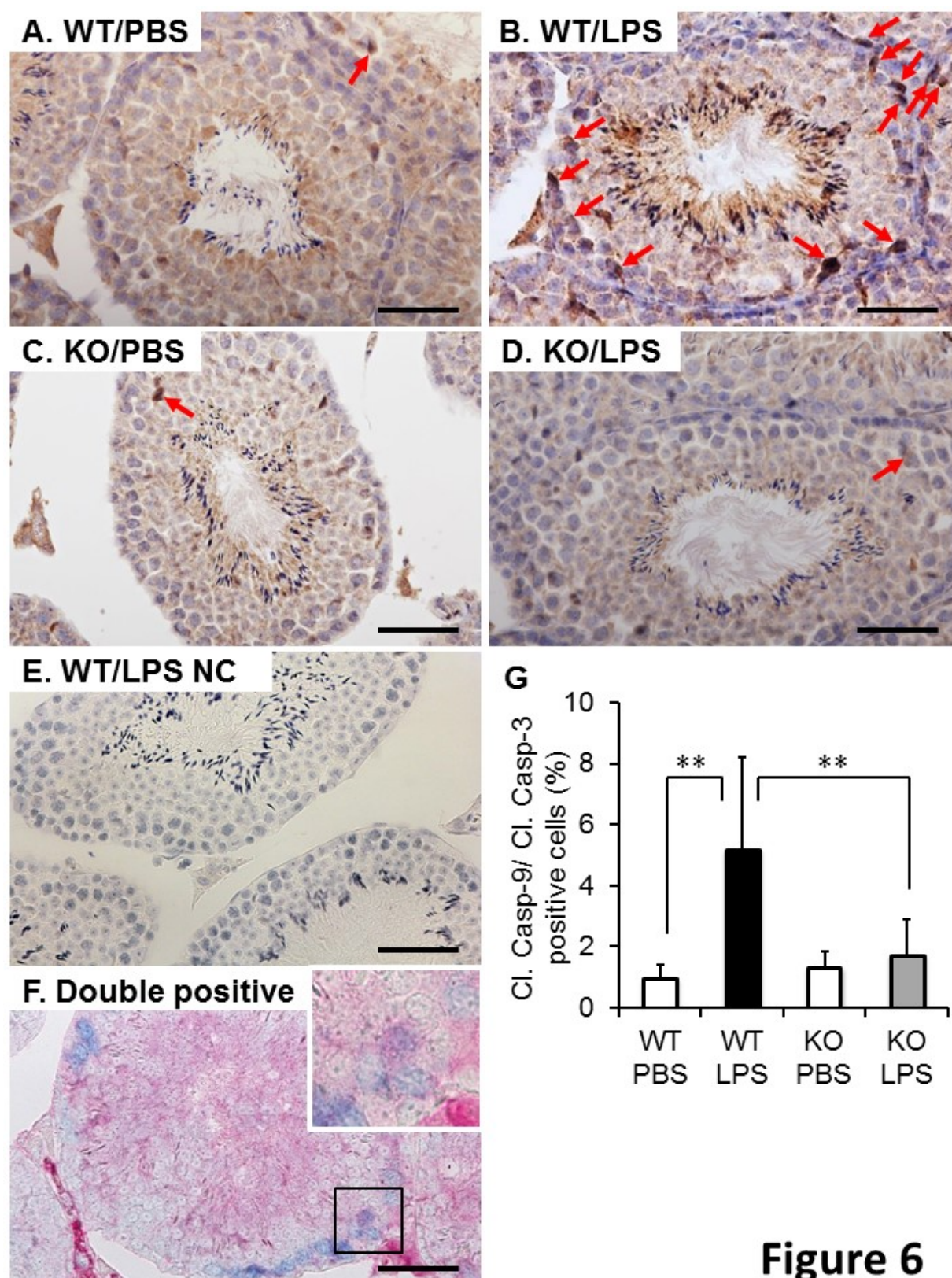
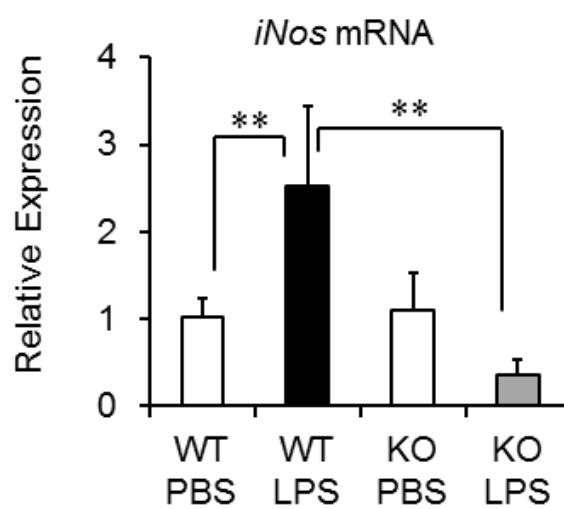


Figure 3

**Figure 4**

**Figure 5**

**Figure 6**

**Figure 7**

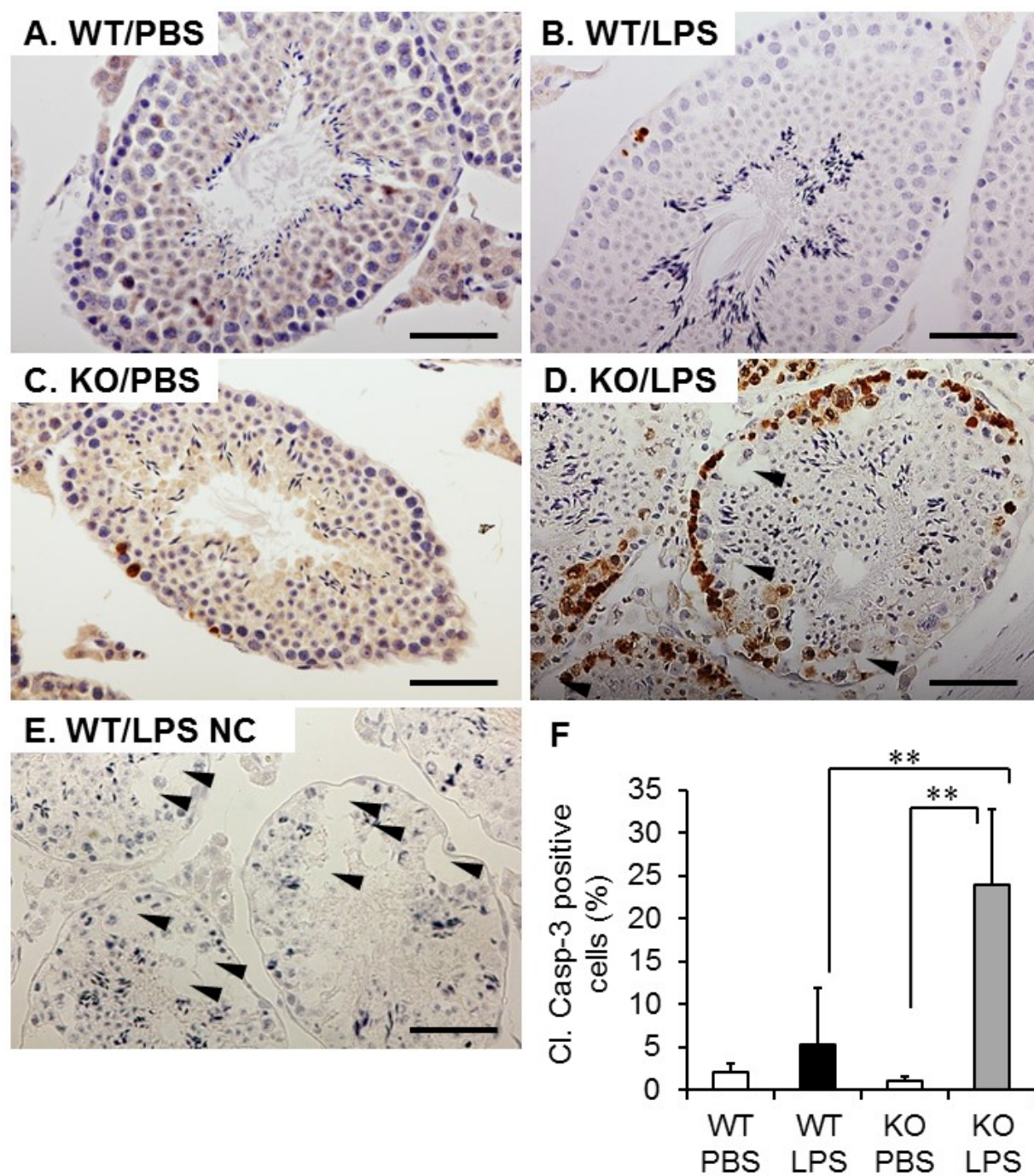


Figure 8

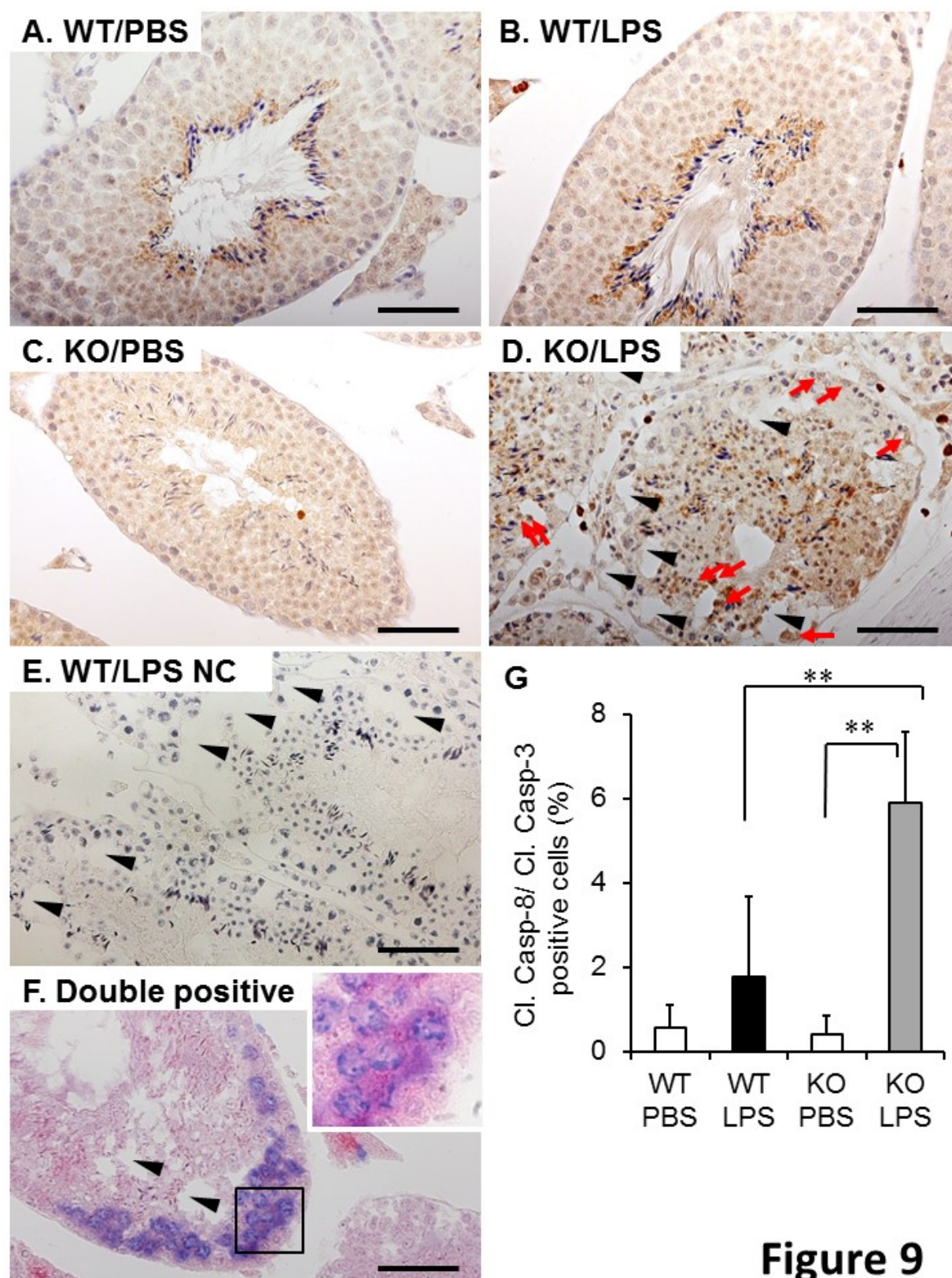


Figure 9

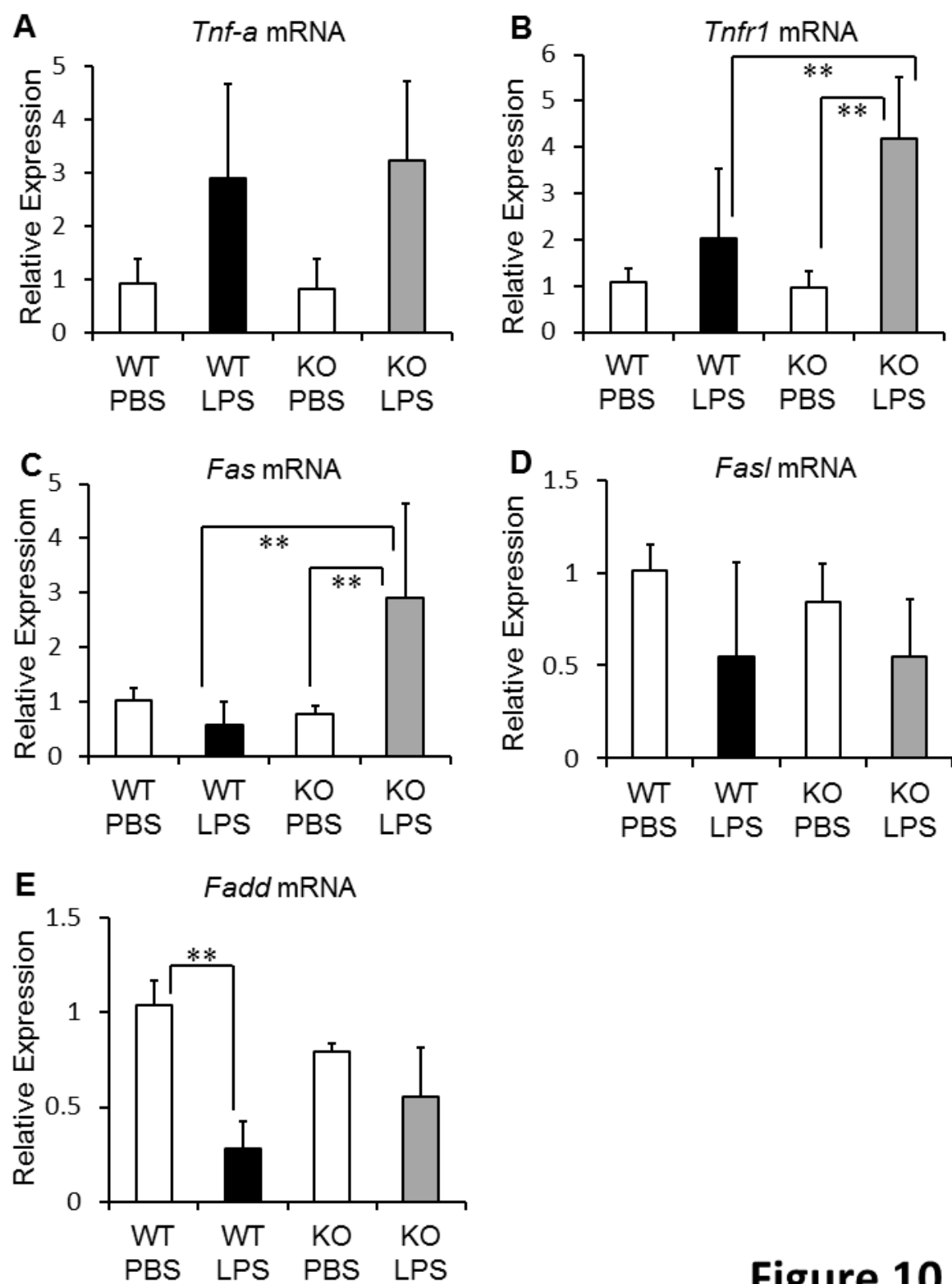
**Figure 10**

Table 1. Quantitative PCR primer sequences and annealing temperatures

Gene	Primer sequence (5' to 3')		annealing
	Forward	Reverse	°C
<i>Tnf-alpha</i>	AGAAGAGGCACTCCCCCAAAA	CCGAAGTTCAGTAGACAGAAGAGCG	63
<i>Tnfr1</i>	AGAACCAGTTCCAACGTACC	TCTGAGTCTCCTTACAGGGGAT	57
<i>Fas</i>	GAACCTCCAGTCGAAACCA	GCTGTGTCTTGGATGCTGTCA	62
<i>Fasl</i>	TCAGTCTTGCAACAACCAGCC	GATTGAATACTGCCCCCAGGT	62
<i>Fadd</i>	CAGGTGGCATTGACATTGTG	ACCGAGGCGTTCTTCTTCTCA	62
<i>iNos</i>	TCCTCACTGGGACAGCACACAGAATG	GTGTCATGCAAAATCTCTCCACTGCC	65.6
<i>Gapdh</i>	TGTGTCCGTCGTGGATCTGA	TTGCTGTTGAAGTCGCAGGAG	60